Malaria Journal

RESEARCH

Open Access

Mapping current and future thermal limits to suitability for malaria transmission by the invasive mosquito *Anopheles stephensi*

Sadie J. Ryan[1*], Catherine A. Lippi[1], Oswaldo C. Villena[2], Aspen Singh[1], Courtney C. Murdock[3] and Leah R. Johnson[4,5,6]

Abstract

Background *Anopheles stephensi* is a malaria-transmitting mosquito that has recently expanded from its primary range in Asia and the Middle East, to locations in Africa. This species is a competent vector of both *Plasmodium falciparum* and *Plasmodium vivax* malaria. Perhaps most alarming, the characteristics of *An. stephensi*, such as container breeding and anthropophily, make it particularly adept at exploiting built environments in areas with no prior history of malaria risk.

Methods In this paper, global maps of thermal transmission suitability and people at risk (PAR) for malaria transmission by *An. stephensi* were created, under current and future climate. Temperature-dependent transmission suitability thresholds derived from recently published species-specific thermal curves were used to threshold gridded, monthly mean temperatures under current and future climatic conditions. These temperature driven transmission models were coupled with gridded population data for 2020 and 2050, under climate-matched scenarios for future outcomes, to compare with baseline predictions for 2020 populations.

Results Using the Global Burden of Disease regions approach revealed that heterogenous regional increases and decreases in risk did not mask the overall pattern of massive increases of PAR for malaria transmission suitability with *An. stephensi* presence. General patterns of poleward expansion for thermal suitability were seen for both *P. falciparum* and *P. vivax* transmission potential.

Conclusions Understanding the potential suitability for *An. stephensi* transmission in a changing climate provides a key tool for planning, given an ongoing invasion and expansion of the vector. Anticipating the potential impact of onward expansion to transmission suitable areas, and the size of population at risk under future climate scenarios, and where they occur, can serve as a large-scale call for attention, planning, and monitoring.

Keywords *Anopheles stephensi*, Malaria, Climate change, Physiological response

*Correspondence:
Sadie J. Ryan
sjryan@ufl.edu
Full list of author information is available at the end of the article

Background

Malaria remains a critical global health challenge, with 241 million cases reported by the World Health Organization (WHO) in 2020 alone [1]. Although the current distribution of malaria is largely pantropical, the overwhelming majority of cases and deaths occur in non-arid regions of Africa, where the WHO estimated approximately 600,000 deaths occurred in 2020 [1–3]. Malarial transmission throughout sub-Saharan Africa is historically attributable to a few key mosquito vectors, most notably those in the *Anopheles gambiae* species complex [1, 4]. However, in 2019 the WHO issued a notice to alert public health authorities to the recent expansion of invasive *Anopheles stephensi* into the Horn of Africa, identifying this new vector species as a major potential threat to malaria control in the region [5–8].

The expansion of *An. stephensi* represents a new critical threat, not only to communities in Africa, but also to global public health. A competent vector of both *Plasmodium falciparum* and *Plasmodium vivax* malaria, *An. stephensi* has been implicated in malaria transmission throughout much of its native range in Asia and the Middle East, including India, Iran, and Pakistan [9–13]. In contrast with other Anopheline species, *An. stephensi* is capable of exploiting containers of standing water for ovipositional habitat, similar to container-breeding mosquitoes in the genus *Aedes*, including *Aedes aegypti* and *Aedes albopictus* [14]. This notable difference in life history has enabled the incursion of *An. stephensi* into built environments, fueling urban outbreaks of malaria and facilitating invasions into new geographic areas. In the past decade, *An. stephensi* has successfully expanded its range into the African continent, with established populations in Djibouti, Ethiopia, and Sudan [15]. Alarmingly, the arrival of this new vector has precipitated epidemics in populations centrally located in urban areas, where rates of malaria have historically been significantly lower compared to rural and peri-urban areas [16]. This shift in underlying risk was exemplified by a notable malaria outbreak in Djibouti City in 2012, where such outbreaks have since become increasingly severe, and are now an annual occurrence [17, 18]. Other physiological adaptations of *An. stephensi*, such as acquired insecticide resistance [19] and greater range of thermal tolerance compared to *An. gambiae* [20], raise further concerns regarding the continued success of this mosquito as an invasive species, and its ability to potentially undermine existing vector control strategies [21]. Perhaps unsurprisingly, *An. stephensi* has been identified as a major risk to malaria elimination targets, with global public health organizations calling for increased entomological surveillance and vector control in areas at imminent risk of invasion [5].

Mapping geographic estimates of transmission suitability can provide essential tools for assessing the current and future risk of *An. stephensi* invasions, and subsequent malaria transmission. A great deal of research has been conducted to delineate the extent of temperature-dependent malaria suitability in Africa [22, 23] and beyond [24–29]. In previous work, malaria transmission suitability for Africa was mapped, using a model comprised of an array of *Anopheles* spp. input parameters, primarily for *P. falciparum* malaria transmitted by *An. gambiae* [30, 31]. In a recently updated model, *An. gambiae* and *An. stephensi*, and the two main malarial parasites they transmit (*P. falciparum* and *P. vivax*), were separately modelled to produce thermal suitability curves for transmission [20, 30]. While the potential geographic dispersal of *An. gambiae* is functionally limited by arid conditions, *An. stephensi* is a container breeder that is resilient to habitat extremes [5]. Therefore, *An. stephensi* is able to thrive in close association with people, and thus potentially able to establish itself everywhere that temperature is not limiting. Thus, understanding the potential areas for suitability for transmission by this invasive mosquito now, and in the future, is important for capacity building and planning control efforts.

In this study, the global suitability of malaria transmission by *An. stephensi* was mapped using modelled thermal limits under current and future climate scenarios. Unlike previous studies to map the distribution of malaria, the projected distributions are not limited to non-arid regions, given the life history of *An. stephensi*, and instead make similar assumptions to those for mapping *Aedes* spp. transmitted diseases. Additionally, *An. stephensi* thermal suitability maps were combined with projected human population density estimates, enabling us to assess not only the areas that are vulnerable to malaria transmission through *An. stephensi* expansions, but also the magnitude of threat in terms of people at risk (PAR).

Methods

Thermal suitability model

In a previous study (Villena et al. [20]), used mechanistic modelling to establish thermal suitability curves for transmission of *P. falciparum* and *P. vivax* by *An. stephensi*. Briefly, thermal response data for vector and parasite pairings were synthesized from published data. These data were used to parameterize a formulation for R_0, the basic reproductive number, that explicitly incorporated temperature-dependent traits for both mosquito vectors and malarial parasites,, building on a model for *P. falciparum* malaria transmission initially described in

Mordecai et al. [32]. The temperature-dependent components of the R_0 formulation were used to define a suitability metric $S(T)$, defined as:

$$S(T) = \left(\frac{a(T)^2 bc(T) e^{-\frac{\mu(T)}{PDR(T)}} EFD(T) P_{EA}(T) MDR(T)}{\mu(T)^3} \right)^{\frac{1}{2}},$$

where a is mosquito biting rate; bc is vector competence; μ is the mosquito mortality rate; PDR is the parasite development rate; EFD is mosquito fecundity expressed as the number of eggs per female per day; P_{EA} is the proportion of eggs surviving to adulthood; and MDR is the mosquito development rate.

A Bayesian approach was used in Villena et al. 2022 to fit unimodal thermal response curves of traits for each mosquito or parasite species [20]. Samples from the resulting joint posterior distribution of the suitability metric were used to calculate overall thermal response, in addition to critical temperature thresholds for pathogen transmission by species [20].

In this study, the thermal boundaries from Villena et al. [20] were used as the basis for mapping thermal suitability, taking values where the malaria transmission suitability metric for *An. stephensi* was greater than zero (S(T) > 0), with a posterior probability greater than 0.975 [20]. The resulting thermal limits for malaria transmitted by *An. stephensi* are temperatures of 16.0–36.5 °C for *P. falciparum* and 16.6–31.7 °C for *P. vivax* [20].

Climate data

In this paper, baseline and future scenarios for *An. stephensi* transmitted *P. falciparum* and *P. vivax* suitability are described. Outputs are presented for a baseline climate scenario, and future potential climate driven outputs for four General Circulation Models (GCMs), following the methodology used in Ryan et al. [33, 34] to describe climate impacts on the global distribution of *Aedes* spp. transmitted diseases.

Baseline and future scenario climate model output data were acquired from the research programme on Climate Change, Agriculture, and Food Security (CCAFS) web portal (http://ccafs-climate.org/data_spatial_downscaling/), part of the Consultative Group for International Agricultural Research (CGIAR). The baseline climate model from which these are projected is the WorldClim v1.4 baseline [35], and thus it serves as the baseline for these models. The CCAFS future model outputs were created using the delta downscaling method, from the IPCC AR5. The GCMs used in this study are the Beijing Climate Center Climate System Model (BCC-CSM1.1); the Hadley GCM (HadGEM2-AO and HadGEM2-ES); and the National Center for Atmospheric Research's Community Climate System Model (CCSM4). The datasets were obtained at a resolution of 5-arc minutes, matching the spatial resolution of baseline data.

For visualizations, one of the General Circulation Models (GCMs) was used: the Hadley Centre Global Environment Model version 2, Earth-System configuration (HADGEM2-ES) under two scenarios for greenhouse gas emissions, or representative concentration pathways (RCPs): RCP 4.5 and RCP 8.5. The Intergovernmental Panel on Climate Change (IPCC) describes RCP 4.5 as a moderate scenario in which emissions peak around 2040 and then decline, while RCP 8.5 is the highest baseline emissions scenario in which emissions continue to rise throughout the twenty-first century. Mechanistic transmission models were projected onto climate data in R (v. 4.1.2) with the package 'raster' [36]. Monthly mean temperatures were thresholded according to the thermal suitability limits for each malaria species, and the number of suitable months of transmission summed (0–12) in a pixel-wise analysis for the globe.

Population data

In order to establish a population baseline, the 2020 Gridded Population of the World (GPW4, ver 4.11) was used [37]. The decision about how to best match climate baselines with population is complex, as baselines represent climate normal periods around the start of the twenty-first century, rather than a 'current' climate baseline. However, in this study, the nearest decade to current conditions for population baseline was chosen. For the future population, 2050 projections for two Shared Socioeconomic Pathways (SSPs) [38, 39] were chosen, best matched to the chosen RCPs. As the combinations of RCPs and SSPs are not all realistic, CMIP5 RCP 4.5 and RCP 8.5 for SSP2 and SSP5, respectively, were modelled. SSP2 represents a "middle of the road" scenario, assuming patterns of social, economic, and technological growth that do not appreciably deviate from historical trends. SSP5 assumes significant investments in health, technology, economic, and social development, coupled with simultaneous exploitation of fossil fuel resources and the adoption of resource-intensive lifestyles. All geographic layers in the analyses were aggregated to a 0.25° grid cell for consistency.

Suitability mapping

Monthly suitability maps were produced for baseline and future climate scenarios (i.e., RCP 4.5 and RCP 8.5), using one GCM (HADGEM-ES) at a near-future time horizon (i.e., 2050), for illustration (Fig. 1). Following the approach of Ryan et al. [34, 40] Maps for figures were created using ArcGIS (ver. 10.1)[41].

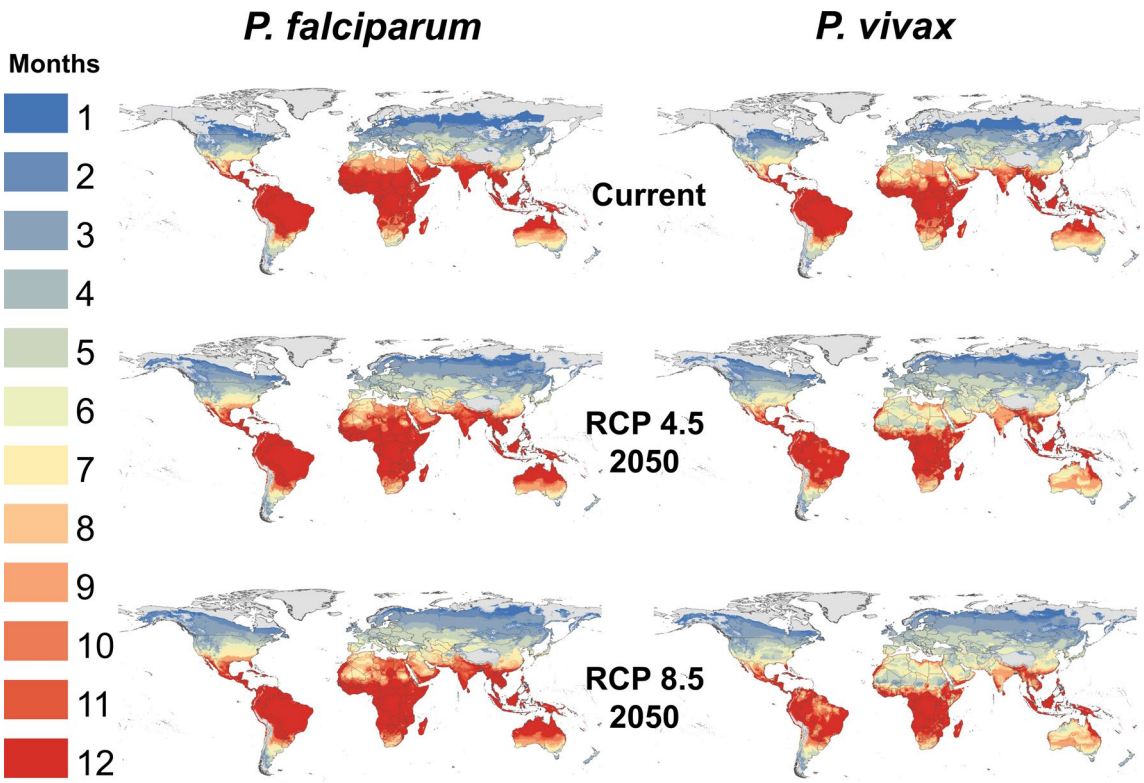

Fig. 1 Thermal suitability for transmission of *P. falciparum* and *P. vivax* malaria by *An. stephensi*. Transmission suitability is shown under current climate conditions, and for the year 2050 at RCP 4.5 and RCP 8.5. The number of months of suitable temperatures are given as shaded areas, where the posterior probability of S(T) > 0 is 0.975

To describe the impact to populations in current and future landscapes, the Global Burden of Disease (GBD) regions [42] were used to summarize the population at risk (PAR). Additional file 1: Tables S1–S4 summarize the top 10 regions, and global gain overall, in terms of increased (difference between current and projected) PAR for both year-round (12 month, endemic), and for 'any' (one or more months), for each of transmission suitability of *P. falciparum* and *P. vivax* by *An. stephensi*, under the two future RCP x SSP scenarios, averaged across the 4 GCMs (also summarized at a global level in Table 1).

Results

Baseline suitability and duration of transmission season

Maps of months of *An. stephensi* malaria transmission suitability for *P. falciparum* and *P. vivax* are shown in Fig. 1. Much of Africa is projected to be suitable at baseline for nearly year-round transmission for both malaria parasites. Beyond Africa, the predicted baseline thermal transmission suitability for both *P. falciparum* and *P. vivax* extends throughout the global tropics, throughout the known existing range of the Middle East, extending throughout Asia, Central America, South America, and marginally in North America. The predicted potential range for year-round transmission suitability of *P. falciparum* extends further North and South than *P. vivax*, with notable extension of the transmission season in northern Africa, the Middle East, India, and central Australia. The narrower thermal suitability bounds for *P. vivax* constrains the baseline potential extent, compared to that for *P. falciparum*. Seasonal transmission suitability at baseline climate conditions is projected to be globally widespread for both *P. falciparum* and *P. vivax*, extending well into temperate regions in North America, Europe, and Asia.

Predicted future suitability

Mapped transmission suitability in 2050, for RCP 4.5 and RCP 8.5 scenarios is shown in Fig. 1. An expansion of the transmission suitability season for *P. falciparum* is seen in both RCPs. Notably, the potential for any transmission (i.e., one or more months) is predicted to expand at northern latitudes, where areas with no current malaria suitability will have the potential for transmission, at least for one month every year. This includes portions of Alaska in the US, northern Canada, Scandinavia, and Russia. The length of the *P. falciparum* transmission

Table 1 People at Risk (PAR) for thermal suitability of transmission of malaria (*P. falciparum* or *P. vivax*) by *Anopheles stephensi*, under a baseline climate, and under two representative concentration pathways (RCP 4.5 and 8.5), across four global circulation model output projections for 2050 (BC: Beijing Climate Center Climate System Model (BCC-CSM1.1); CC: National Center for Atmospheric Research's Community Climate System Model (CCSM4); HD: Hadley GCM HadGEM2-AO; HE: Hadley GCM HADGEM2-ES), paired with shared socioeconomic pathway projections of population (RCP 4.5 × SSP2; RCP 8.5 × SSP5), for 2050. These are given for Year-round transmission suitability (12 months), and for one or more months of suitability

RCP	GCM	Year-round		One or more months	
		P. falciparum	*P. vivax*	*P. falciparum*	*P. vivax*
BASELINE	BASELINE	2,978,746,847	2,097,002,867	7,449,067,483	7,383,343,414
RCP 4.5	BC	3,774,756,103	2,127,908,652	8,750,860,448	8,728,473,114
	CC	4,054,286,646	2,252,417,759	8,753,397,990	8,736,201,422
	HD	3,805,562,194	1,974,878,300	8,771,619,653	8,755,597,360
	HE	3,736,169,575	2,021,833,976	8,772,921,907	8,757,997,413
RCP 8.5	BC	3,166,706,402	1,743,224,294	8,177,804,060	8,165,124,757
	CC	3,307,469,096	1,813,969,917	8,177,578,312	8,163,138,249
	HD	3,361,036,908	1,732,882,405	8,181,652,270	8,170,347,061
	HE	3,164,609,570	1,530,848,172	8,185,991,009	8,180,851,173

season is expected to increase in temperate regions of North America and Europe, southern Africa, and in central Australia. Yet, changing climate conditions will shorten the length of the *P. falciparum* transmission season in some areas, most notably in northern Africa, the Middle East, and northern India. The transmission suitability for *P. vivax* is also predicted to extend further North in the future, encroaching on areas that do not currently experience malaria transmission. The length of the *P. vivax* transmission season is expected to increase in southern Africa and in parts of North America, including Mexico and along the Gulf Coast in the US. There are also marked decreases in the length of the *P. vivax* transmission season, most notably throughout northern Africa, the Middle East, India, Asia, northern Australia, and South America. Raster output for additional scenarios of future climate change from this study is available on the Harvard Dataverse.

Population at risk

The projections of thermal suitability for transmission of *P. falciparum* and *P. vivax* by AS for the two future scenarios of RCP 4.5 and RCP 8.5, in combination with matched population projections SSP2 and SSP5, respectively, revealed that in many regions of the world, increases in people at risk of transmission suitability will occur (Additional file 1: Tables S1-S4). The prediction for SSP2 population for the globe is larger than SSP5 in 2050 (9.17 billion vs 8.56 billion [43]), this reflects the combination of potential geographic shifts of suitability and the underlying population changes. Perhaps counterintuitively, the RCP 4.5 scenario predicts a larger net increase than RCP 8.5, for PAR in both 'any' (one or more) transmission, and year-round (endemic) transmission scenarios (Table 1). The baseline and net global future population at risk (PAR) for transmission suitability across the 4 GCMs are given in Table 1, comparing *P. falciparum* and *P. vivax* suitability.

At 2020 population baseline, 7.45 billion people are predicted to be at risk for transmission suitability for one or more months for *P. falciparum* in *An. stephensi*, and 7.38 billion for *P. vivax* in AS. Under RCP 4.5, the net PAR for *P. falciparum* suitability increases to a range of 8.75–8.77 billion, and for *P. vivax* 8.73–8.76 billion, across the 4 GCMs; and under RCP 8.5, the estimated PAR for *P. falciparum* suitability is 8.18–8.19 billion, and for *P. vivax* 8.16–8.18 billion (Table 1).

At baseline, the year-round PAR for *P. vivax* is 2.13 billion people, while it is 3.77 billion for *P. falciparum*, emphasizing the difference in risk imposed by the broader temperature range of suitability for *P. falciparum*. Under RCP 4.5, the net PAR for *P. falciparum* suitability increases to a range of 3.73–4.05 billion, and 1.98–2.25 billion for *P. vivax*. Under RCP 8.5 conditions, net par for *P. falciparum* suitability increases to 3.16–3.36 billion, and 1.53–1.81 billion for *P. vivax*.

The top 10 largest regional increases in PAR for each of *P. falciparum*, *P. vivax*, and for year-round and 'any' transmission are given in Additional file 1: Tables S1-4, including the global gains in increases (in contrast to net changes). For *P. falciparum*, for endemic (year-round) transmission PAR increases, East and West Sub-Saharan Africa regions are the top two affected, under both the RCP 4.5 and RCP 8.5 scenario (Additional file 1: Table S1); for *P. vivax*, while East sub-Saharan Africa is also the top affected region, the second place is Central

African Region, indicating a shifted geographic impact with the narrower thermal bounds (Additional file 1: Table S2). For 'any' (one or more months) transmission suitability, South Asia region is the top affected for both *P. falciparum* and *P. vivax*, ahead of East sub-Saharan Africa region, suggesting a shift of seasonal, sub-endemic risk into high density population areas in both of the future scenarios explored here (Additional file 1: Tables S3, S4).

Discussion

Assessing the future risk of *An. stephensi* expansion against the backdrop of changing climate is imperative for public health planning and risk mitigation. Its propensity to spread and establish outside of its current range is already underway, drawing the attention of the global health community [5, 7, 18, 44]. As a malaria transmitting Anopheline capable of exploiting a similar niche to the urban adapted *Aedes* spp. mosquitoes, anticipating where the bounds of thermal limits to persistence and transmission exist is a step towards understanding where it can invade and establish, both now and in the future.

Using a recently published thermal suitability model for transmission of both *P. falciparum* and *P. vivax* malaria by *An. stephensi* [20], mapped months of suitability demonstrated that a large part of the world is already suitable for one or more months of the year, putting an estimated 7.38–7.45 billion people at risk of that potential. While the actual arrival, establishment, and onwards transmission of malaria may be less risky for areas with a low number of months of suitability, this approach indicates that a baseline of 2.13–3.77 billion people are currently living in places with endemic risk—not simply in the known existing range for transmission by *An. stephensi*. The potential for future shifts in the range of suitable areas was explored, as a function of a changing climate and shifting population projections, reflective of those potential climate scenarios. The mapped number of months of transmission suitability showed a poleward expansion of areas becoming suitable, and a shift from some lower latitude locations to becoming hotter than suitable for transmission during parts of the year, shortening the season. While this shift away from suitability results in predicted declines in risk to populations, as transmission suitability shifts out of hotter regions, other health crises are exacerbated at overly high temperatures [45–48], and this is thus not cause for less alarm, nor is it mitigation for malaria.

This exploration of potential future climate impacts on a vector currently expanding its range is based on current vector-pathogen biology and thermal limits to the life-history of *An. stephensi* and the malaria parasites. The conditions under which parameters in the underlying thermal suitability model were established were idealized laboratory conditions, and are not yet established for *An. stephensi* undergoing the climate changes modelled here. The environment experienced in a changed climate in 2050 may induce different interactions between vectors and their pathogens, but the plastic responses of the vector (e.g. urban adaptation, behavioral avoidance of environmental extremes) and the pathogen (e.g. rapid evolution under novel environmental pressures, or fluctuating temperatures), and how that will impact the vector microbiome [49], potentially altering vector competence, will lead to broader potential temperature limits to suitability, making the estimates presented here conservative. Further, these projections only consider malaria transmission in terms of extrinsic incubation (i.e., development in the mosquito) and transmission to the host. This does not include the human stages of malaria development, and some malarial parasites have adaptations, such as hypnozoites for *P. vivax* [50], which can leverage human reservoirs beyond the environmental bounds of transmission suitability in adult mosquitoes. Conversely, these estimates may represent a "worst case" scenario. Model output at the global scale may oversimplify local effects that protect against mosquito invasion, and likewise this study cannot account for the potentially mitigating effects of rapid interventions and successful malaria control initiatives. This underscores the importance of expanding surveillance capacity for the early detection and rapid elimination of expanding *An. stephensi* populations to reduce PAR in the future, particularly in countries neighboring current areas of expansion.

A knock-on effect of the potential expansion of a novel, urban-adapted, malaria vector into, for example, the Americas, is that adding a competent malaria vector to areas with existing competent malaria vectors expands the competent vector community. This compounds the risk in a changing world for facilitating spillover from a novel invader experiencing perhaps only a shortened suitability season to established Anopheline species (e.g. *Anopheles quadrimaculatus* in parts of N. America).

The ongoing expansion of *An. stephensi* is troubling, given its implication in the shift from primarily rural to urban malaria transmission. The mapped risk projections in this study, though global in extent, will be useful to local governments and agencies for planning broad-scale vector control and resource allocation efforts. Potential vulnerability to invasion is useful information for decision making and policy formation, particularly for countries at the forefront of *An. stephensi* expansion,

neighbouring current locations where the vector has been documented. The successful expansion and establishment of invasive urban mosquitoes is mediated by many factors beyond the scope of these models, such as introduction pathway, frequency of travel, and individual water storage practices [51, 52]. Thus, these results demonstrate the need for increased surveillance activities in areas at risk of transmission, but importantly, underscore the need for timely sharing and dissemination of known distribution data. Although urban malaria transmission represents a new threat for many existing vector control programmes to manage, there may be opportunities for the formation of successful mitigation efforts, given that agencies are aware of potential expansion. With enough lead time, mosquito control agencies may be able to successfully leverage knowledge, experience, and tools for controlling other urban container-breeding mosquitoes to suppress the proliferation of invasive *An. stephensi* [6]. For example, dengue fever surveillance and control programmes that target *Ae. aegypti* may have the capacity to expand efforts to include *An. stephensi* without a major investment in novel resources. Though there are still challenges in programme adaptation, such as the need to address insecticide resistance, it is likely that effective control measures will not have to be designed from the ground up.

Conclusion

Mapping thermal suitability for malaria transmission for the invasive urban-adapted *An. stephensi* for baseline and future climate and population projection scenarios shows that much of the world is suited to continued range expansion now and into the future. While this work demonstrates that around a third of the world's population lives in areas of potential risk, understanding where range expansion is plausible, and how that may shift in the future, provides broad scale tools for motivating surveillance and opportunities for preemptive interventions. Of key importance, the similarity between *An. stephensi* and *Aedes* spp, and their management as urban container breeders may provide an opportunity to leverage existing vector management and control for *An. stephensi*.

Abbreviations

CGIAR	Consultative Group for International Agricultural Research
CMIP	Climate Model Intercomparison Project
GCM	General Circulation Model
GPW	Gridded Population of the World
RCP	Representative Concentration Pathway
SSP	Shared Socioeconomic Pathway
WHO	World Health Organization

Supplementary Information

The online version contains supplementary material available at https://doi.org/10.1186/s12936-023-04531-4.

Additional file 1. Table S1. Top 10 Global Burden of Disease defined regional increase in people at risk (PAR) for year-round transmission suitability of P. falciparum by *An. stephensi* in 2050, under RCP 4.5 (SSP2 population projection) and RCP 8.5 (SSP5 population projection) future climate scenarios, averaged across four general circulation models (GCMs) as described in the main methods. Global increase is the sum of all gains in PAR increases across all GBD regions. **Table S2.**Top 10 Global Burden of Disease defined regional increase in people at risk (PAR) for year-round transmission suitability of *P. vivax* by *An. stephensi* in 2050, under RCP 4.5 (SSP2 population projection) and RCP 8.5 (SSP5 population projection) future climate scenarios, averaged across four general circulation models (GCMs) as described in the main methods. Global increase is the sum of all gains in PAR increases across all GBD regions. **Table S3.**Top 10 Global Burden of Disease defined regional increase in people at risk (PAR) for one or months transmission suitability of *P. falciparum* by *An. stephensi* in 2050, under RCP 4.5 (SSP2 population projection) and RCP 8.5 (SSP5 population projection) future climate scenarios, averaged across four general circulation models (GCMs) as described in the main methods. Global increase is the sum of all gains in PAR increases across all GBD regions. **Table S4.**Top 10 Global Burden of Disease defined regional increase in people at risk (PAR) for one or months transmission suitability of *P. vivax* by *An. stephensi* in 2050, under RCP 4.5 (SSP2 population projection) and RCP 8.5 (SSP5 population projection) future climate scenarios, averaged across four general circulation models (GCMs) as described in the main methods. Global increase is the sum of all gains in PAR increases across all GBD regions.

Acknowledgements

The authors would like to acknowledge the thoughtful insights of our anonymous reviewers.

Author contributions

SJR, CAL and AS conducted analyses; SJR and CAL drafted the paper, figures and tables. All authors contributed to the final version. All authors read and approved the final manuscript.

Funding

SJR, CAL, and LRJ were supported by CIBR: VectorByte: A Global Informatics Platform for studying the Ecology of Vector-Borne Diseases NSF DBI 2016265; LRJ was additionally supported by NSF DMS/DEB 1750113 and NIH R01AI122284.

Availability of data and materials

All model output rasters are available through Harvard Dataverse (https://dataverse.harvard.edu/dataverse/stephensimaps), all climate layers used are freely available online and described within the paper. R Code for creating model outputs is available publicly on GitHub (https://github.com/RyanLab/stephensimaps).

Declarations

Ethics approval and consent to participate

Not applicable.

Consent for publication

Not applicable.

Competing interests

The authors declare no competing interests.

Author details

[1]Department of Geography and Emerging Pathogens Institute, University Florida, Gainesville, FL 32611, USA. [2]The Earth Commons Institute, Georgetown

University, Washington, DC 20007, USA. [3]Department of Entomology, College of Agriculture and Life Sciences, Cornell University, Ithaca, NY, USA. [4]Department of Statistics, Virginia Tech, Blacksburg, VA, USA. [5]Computational Modeling and Data Analytics, Virginia Tech, Blacksburg, VA, USA. [6]Department of Biology, Virginia Tech, Blacksburg, VA, USA.

Received: 20 December 2022 Accepted: 13 March 2023
Published online: 21 March 2023

References

1. WHO. World malaria report 2021. Geneva, World Health Organization; 2021.
2. Coetzee M. Distribution of the African malaria vectors of the *Anopheles gambiae* complex. Am J Trop Med Hyg. 2004;70:103–4.
3. Hay SI, Guerra CA, Tatem AJ, Noor AM, Snow RW. The global distribution and population at risk of malaria: past, present, and future. Lancet Infect Dis. 2004;4:327–36.
4. Sinka ME, Bangs MJ, Manguin S, Coetzee M, Mbogo CM, Hemingway J, et al. The dominant *Anopheles* vectors of human malaria in Africa, Europe and the Middle East: occurrence data, distribution maps and bionomic précis. Parasit Vectors. 2010;3:117.
5. WHO. Vector alert: *Anopheles stephensi* invasion and spread. Geneva, World Health Organization; 2019. Report No.: WHO/HTM/GMP/2019.09. https://www.who.int/news-room/detail/26-08-2019-vector-alert-anopheles-stephensi-invasion-and-spread
6. Allan R, Budge S, Sauskojus H. What sounds like *Aedes,* acts like *Aedes,* but is not *Aedes*? Lessons from dengue virus control for the management of invasive *Anopheles*. Lancet Global Health. 2023;11:e165–9.
7. Mnzava A, Monroe AC, Okumu F. *Anopheles stephensi* in Africa requires a more integrated response. Malar J. 2022;21:156.
8. Tadesse FG, Ashine T, Teka H, Esayas E, Messenger LA, Chali W, et al. *Anopheles stephensi* Mosquitoes as Vectors of *Plasmodium vivax* and *falciparum*, Horn of Africa, 2019. Emerg Infect Dis. 2021;27:603–7.
9. Sharma SK, Hamzakoya KK. Geographical spread of *Anopheles stephensi*, vector of urban malaria, and *Aedes aegypti*, vector of dengue/DHF, in the Arabian Sea Islands of Lakshadweep. India Dengue Bull. 2001;25:88–91.
10. Sumodan PK, Kumar A, Yadav RS. Resting behavior and malaria vector incrimination of *Anopheles stephensi* in Goa. India J Am Mosq Control Assoc. 2004;20:317–8.
11. Manouchehri AV, Javadian E, Eshighy N, Motabar M. Ecology of *Anopheles stephensi* Liston in southern Iran. Trop Geogr Med. 1976;28:228–32.
12. Pervez SD, Shah IH. Role of *Anopheles stephensi* as malaria vector in rural area of Pakistan. Pak J Health. 1989;26:73–84.
13. Gayan Dharmasiri AG, Perera AY, Harishchandra J, Herath H, Aravindan K, Jayasooriya HTR, et al. First record of *Anopheles stephensi* in Sri Lanka: a potential challenge for prevention of malaria reintroduction. Malar J. 2017;16:326.
14. Mariappan T, Thenmozhi V, Udayakumar P, Bhavaniumadevi V, Tyagi BK. An observation on breeding behaviour of three different vector species (*Aedes aegypti* Linnaeus 1762, *Anopheles stephensi* Liston 1901and *Culex quinquefasciatus* Say 1823) in wells in the coastal region of Ramanathapuram district, Tamil Nadu. India Int J Mosq Res. 2015;2:42–4.
15. Sinka ME, Pironon S, Massey NC, Longbottom J, Hemingway J, Moyes CL, et al. A new malaria vector in Africa: predicting the expansion range of and identifying the urban populations at risk. Proc Natl Acad Sci USA. 2020;117:24900–8.
16. Doumbe-Belisse P, Kopya E, Ngadjeu CS, Sonhafouo-Chiana N, Talipouo A, Djamouko-Djonkam L, et al. Urban malaria in sub-Saharan Africa: dynamic of the vectorial system and the entomological inoculation rate. Malar J. 2021;20:364.
17. Faulde MK, Rueda LM, Khaireh BA. First record of the Asian malaria vector *Anopheles stephensi* and its possible role in the resurgence of malaria in Djibouti. Horn of Africa Acta Trop. 2014;139:39–43.
18. Seyfarth M, Khaireh BA, Abdi AA, Bouh SM, Faulde MK. Five years following first detection of *Anopheles stephensi* (Diptera: Culicidae) in Djibouti, Horn of Africa: populations established—malaria emerging. Parasitol Res. 2019;118:725–32.
19. Yared S, Gebressielasie A, Damodaran L, Bonnell V, Lopez K, Janies D, et al. Insecticide resistance in *Anopheles stephensi* in Somali Region, eastern Ethiopia. Malar J. 2020;19:180.
20. Villena OC, Ryan SJ, Murdock CC, Johnson LR. Temperature impacts the environmental suitability for malaria transmission by *Anopheles gambiae* and *Anopheles stephensi*. Ecology. 2022;103: e3685.
21. Chakraborty M, Ramaiah A, Adolfi A, Halas P, Kaduskar B, Ngo LT, et al. Hidden genomic features of an invasive malaria vector, *Anopheles stephensi*, revealed by a chromosome-level genome assembly. BMC Biol. 2021;19:28.
22. Weiss DJ, Bhatt S, Mappin B, Van Boeckel TP, Smith DL, Hay SI, et al. Air temperature suitability for *Plasmodium falciparum* malaria transmission in Africa 2000–2012: a high-resolution spatiotemporal prediction. Malar J. 2014;13:171.
23. Craig MH, Snow RW, le Sueur D. A climate-based distribution model of malaria transmission in sub-Saharan Africa. Parasitol Today. 1999;15:105–11.
24. Kiszewski A, Mellinger A, Spielman A, Malaney P, Sachs SE, Sachs J. A global index representing the stability of malaria transmission. Am J Trop Med Hyg. 2004;70:486–98.
25. Guerra CA, Howes RE, Patil AP, Gething PW, Van Boeckel TP, Temperley WH, et al. The international limits and population at risk of *Plasmodium vivax* transmission in 2009. PLoS Negl Trop Dis. 2010;4: e774.
26. Hay SI, Guerra CA, Gething PW, Patil AP, Tatem AJ, Noor AM, et al. A world malaria map: *Plasmodium falciparum* endemicity in 2007. PLoS Med. 2009;6: e1000048.
27. Gething PW, Patil AP, Smith DL, Guerra CA, Elyazar IRF, Johnston GL, et al. A new world malaria map: *Plasmodium falciparum* endemicity in 2010. Malar J. 2011;10:378.
28. Bhattarai S, Blackburn JK, Ryan SJ. Malaria transmission in Nepal under climate change: anticipated shifts in extent and season, and comparison with risk definitions for intervention. Malar J. 2022;21:390.
29. Whittaker C, Hamlet A, Sherrard-Smith E, Churcher TS. Seasonal dynamics of *Anopheles stephensi* and its implications for mosquito detection and emergent malaria control in the Horn of Africa. Proc Natl Acad Sci USA. 2023;120: e2216142120.
30. Ryan SJ, McNally A, Johnson LR, Mordecai EA, Ben-Horin T, Paaijmans K, et al. Mapping physiological suitability limits for malaria in Africa under climate change. Vector Borne Zoonotic Dis. 2015;15:718–25.
31. Ryan SJ, Lippi CA, Zermoglio F. Shifting transmission risk for malaria in Africa with climate change: a framework for planning and intervention. Malar J. 2020;19:170.
32. Mordecai EA, Paaijmans KP, Johnson LR, Balzer C, Ben-Horin T, de Moor E, et al. Optimal temperature for malaria transmission is dramatically lower than previously predicted. Ecol Lett. 2013;16:22–30.
33. Ryan SJ, Carlson CJ, Mordecai EA, Johnson LR. Global expansion and redistribution of *Aedes*-borne virus transmission risk with climate change. PLoS Negl Trop Dis. 2019;13: e0007213.
34. Ryan SJ, Carlson CJ, Tesla B, Bonds MH, Ngonghala CN, Mordecai EA, et al. Warming temperatures could expose more than 1.3 billion new people to Zika virus risk by 2050. Glob Chang Biol. 2021;27:84–93.
35. Fick SE, Hijmans RJ. WorldClim 2: new 1-km spatial resolution climate surfaces for global land areas. Int J Climatol. 2017;37:4302–15.
36. Hijmans RJ, van Etten J. raster: Geographic analysis and modeling with raster data. 2022; https://cran.r-project.org/web/packages/raster
37. Center for International Earth Science Information Network (CIESIN) Columbia University. Gridded Population of the World, Version 4 (GPWv4). US NASA Socioeconomic Data and Applications Center (SEDAC); 2016. http://sedac.ciesin.columbia.edu/data/set/gpw-v4-population-count-adjusted-to-2015-unwpp-country-totals
38. Jones B, O'Neill BC. Global Population Projection Grids Based on Shared Socioeconomic Pathways (SSPs), 2010–2100. NASA Socioeconomic Data and Applications Center (SEDAC); 2017. https://doi.org/10.7927/H4RF5S0P
39. Jones B, O'Neill BC, Gao J. Global One-Eighth Degree Population Base Year and projection grids for the Shared Socioeconomic Pathways (SSPs), Revision 01. Palisades, New York: Palisades, NY: NASA Socioeconomic Data and Applications Center (SEDAC); 2020. https://doi.org/10.7927/m30p-j498
40. Shocket MS, Ryan SJ, Mordecai EA. Temperature explains broad patterns of Ross River virus transmission. Elife. 2018;7: e37762.

41. Esri. ArcGIS Desktop: Release 10. Redlands, CA: Environmental Systems Research Institute.; 2011.
42. Moran AE, Oliver JT, Mirzaie M, Forouzanfar MH, Chilov M, Anderson L, et al. Assessing the Global Burden of Ischemic Heart Disease: Part 1: methods for a systematic review of the global epidemiology of ischemic heart disease in 1990 and 2010. Glob Heart. 2012;7:315–29.
43. Kc S, Lutz W. The human core of the shared socioeconomic pathways: population scenarios by age, sex and level of education for all countries to 2100. Glob Environ Change. 2017;42:181–92.
44. Takken W, Lindsay S. Increased threat of urban malaria from *Anopheles stephensi* mosquitoes. Africa Emerg Infect Dis. 2019;25:1431–3.
45. D'Amato G, Holgate ST, Pawankar R, Ledford DK, Cecchi L, Al-Ahmad M, et al. Meteorological conditions, climate change, new emerging factors, and asthma and related allergic disorders. A statement of the World Allergy Organization. World Allergy Organ J. 2015;8:25.
46. Vicedo-Cabrera AM, Scovronick N, Sera F, Royé D, Schneider R, Tobias A, et al. The burden of heat-related mortality attributable to recent human-induced climate change. Nat Clim Chang. 2021;11:492–500.
47. Burkart KG, Brauer M, Aravkin AY, Godwin WW, Hay SI, He J, et al. Estimating the cause-specific relative risks of non-optimal temperature on daily mortality: a two-part modelling approach applied to the Global Burden of Disease Study. Lancet. 2021;398:685–97.
48. Ebi KL, Capon A, Berry P, Broderick C, de Dear R, Havenith G, et al. Hot weather and heat extremes: health risks. Lancet. 2021;398:698–708.
49. de Angeli DD, Salloum PM, Poulin R. Vector microbiome: will global climate change affect vector competence and pathogen transmission? Parasitol Res. 2023;122:11–7.
50. Mikolajczak SA, Vaughan AM, Kangwanrangsan N, Roobsoong W, Fishbaugher M, Yimamnuaychok N, et al. *Plasmodium vivax* liver stage development and hypnozoite persistence in human liver-chimeric mice. Cell Host Microbe. 2015;17:526–35.
51. Ahn J, Sinka M, Irish S, Zohdy S. Modeling marine cargo traffic to identify countries in Africa with greatest risk of invasion by *Anopheles stephensi*. Sci Rep. 2023;13:876.
52. Swan T, Russell TL, Staunton KM, Field MA, Ritchie SA, Burkot TR. A literature review of dispersal pathways of *Aedes albopictus* across different spatial scales: implications for vector surveillance. Parasit Vectors. 2022;15:303.

Publisher's Note